Electrical MHD Flow of a Nano fluid over Stretching Sheet in the presence of Radiation and Chemical Reaction Effects

S. Sreedhar[1]*, Department of Mathematics, GITAM Institute of Science,
GITAM University, Visakhapatnam, (A.P), India.
S.K. Prasanna Lakshmi[2], Department of Mathematics, GITAM Institute of Science,
GITAM University, Visakhapatnam, (A.P), India.
S.V.V. Rama Devi[3], Department of Mathematics, Raghu Engineering College(A),
Visakhapatnam. (A.P), India.
*Corresponding Author

ABSTRACT

An investigation has been carried out to study the electrical magnetohydrodynamics (EMHD) flow of a nanofluid towards nonlinear stretched surface in the presence of the radiation and chemical reaction effects. The characteristics of heat transfer are analyzed with the electric field and variable thickness phenomenon. The governing equations are transformed to ordinary differential equations by similarity transformation and solved numerically by the Runge-Kutta fourth order method in association with quasi-linear shooting technique. The results are analyzed for the velocity, temperature and concentration fields are presented graphically and discussed qualitatively.

Keywords: MHD, Radiation, Chemical Reaction, Skin friction

INTRODUCTION

Nanofluids is the term coined by Choi [1] to describe the new class of nanotechnology-based heat transfer fluids that exhibit thermal properties superior to those of their host fluids or conventional particle fluid suspensions. Ultra high-performance cooling is one of the most vital needs of many industrial technologies in today's modern world of sophisticated devices and scientific achievements. Nanofluids, in which nano-sized particles (typically less than 100 nanometers) suspended in liquids, have emerged as a potential candidate for the design of heat transfer fluids. Nano is a prefix meaning one-billionth, so a nanometer is one billionth of a meter. The goal of nanofluids is to achieve the highest possible thermal properties at the smallest possible concentrations by uniform dispersion and stable suspension of nanoparticles in host fluids. When used as coolants, nanofluids can provide dramatic improvements in the thermal properties of host fluids. The novel nanofluids enable a more efficient, effective and uniform heat removal capability for systems requiring highly accurate temperature control at high heat fluxes. In view, many authors [2-5] have recently studied the MHD effects on flow problems with differentaspects. They found that, MHD effect have a significant role in thermal management applications. The flow due to stretching boundary layer has extensive coverage in the extrusion a process involves in plastic and metal industries. Magnetohydrodynamic nanofluid is very important in the area of science, engineering and technology.

Considering variable thickness due to flow, it has gained consideration due to widely advances recently in the area of engineeringenhancement in the fields of mechanical, civil, architectural etc [6-8]. This is rooted in theinnovative work of Fang et al. [9] against variable thickness using pure fluid. The surfacemediums of variable thickness have influential values and significant noticed in industrial andengineering processes. It aims at reducing the heaviness of supplementary component andenhances the operation of devices. Consequently,

this drew the attention of various researchers [10-15] for flow behavior against stretching sheet involving variable thickness. Such consideration many several usages in deigns, marine, mechanical, aeronautical and civil engineering. The study of heat and mass transfer with chemical reaction is very crucial in hydrometallurgies and chemical industries. The steady laminar motion of nanofluid past an expanding sheet under the influence Brownian motion and thermophoresis has been studied by Hayat et al [16]. The motion and nanoparticle transfer of heat characteristics of nanofluid over an expanding/shrinking sheet under convective boundary condition has been investigated by Mansur and Ishak [17]. Influence of slip flow and magnetic field on boundary layer motion of alumina/water nanofluid within an annular microchannel with Brownian motion and thermophoresis impact has been analyzed by Malvandi and Ganji [18]. Effects of chemical reaction and partial slip on the three-dimensional flow of a nanofluid impinging on an exponentially stretching surface has been investigated by Gireesha et al. [19].

In this study, we have motivated by theabove-referenced investigation and the vast possible industrialand engineering applications. It has been noticed that the heatand mass transfer work in the past has been mostly dealt with a linearlystretching sheet. Very few studies in this direction are madeusing a nonlinearly stretching sheet. However, no attempt isyet present for the nonlinear stretching sheet with variablethickness for electrical magnetohydrodynamic (EMHD)boundary layer flow of nanofluid with combined influence ofthe thermal radiation, viscous dissipation, Joule heating and chemical reaction. Thiswork introduces such variable thickness on a nonlinearlystretching sheet on electrical magnetohydrodynamic (EMHD) boundary layer flow of a nanofluidover in the literature. This variable thickness of a nonlinear stretchingsheet has extreme coverage in mechanical, civil, aeronauticalstructure and marine engineering designs. The presentationdiscusses the flow of a nanofluid over a nonlinearly stretchingsheet with a variable thickness on electrical magnetohydrodynamic (EMHD) in the presence of thermal radiation, viscousdissipation and Joule heating incorporating Brownian motion, chemical reactionand thermophoresis in the model. The governing equations aretransformed using a set of dimensionless variables and thensolved numerically using Runge-Kutta method along with shooting technique. Numerical solutions are then obtained and investigated in detail for different interesting parameters such as the local skin-friction, Nusselt number and Sherwood number as well as other parameter values such as the velocity, temperature and concentration profiles are presented graphically and discussed qualitatively.

MATHEMATICAL FORMULATION

Consider a two-dimensional steady electrical magnetohydrodynamic (EMHD) nanofluid over a nonlinearly stretching sheet with variable thickness. The velocity of the stretching sheet is denoted as $U_w(x) = U_0(x+b)^n$, and the surface is taken at $y = A(x+b)^{\frac{1-n}{2}}$, in which for $n = 1$ the stretching sheet is of the same thickness. Let us consider the Cartesian coordinate system such that $x-$ axis is chosen along the stretching sheet and $y-$ axis denotes the normal to the stretching sheet, u and v are the velocity components of the fluid in the x and $y-$ directions. The boundary layer equations of the fluid flow are the composition of the continuity equation, the momentum equation, energy equation and concentration equation, which are formulated based on Maxwell's equation and Ohm's law in the presence of Electrical Magneto-Fluid Dynamics (EMHD). The incompressible viscous fluid flow in the presence of an applied magnetic field B and electric field E is taken into the consideration. The flow is due to the stretching of a sheet from a slot through two equal and opposite force and thermally radiative. Magnetic field and the electric field of strength

$B(x)$ and $E(x)$ are applied normal to the flow, such that the Reynolds number is selected small. The induced magnetic field is smaller to the applied magnetic field. Hence the induced magnetic field is absence for small magnetic Reynolds number.

Let usassumed be the less temperature gradient within the viscous fluid flow in such a way that T^4 can be expressed as a linear function of a temperature. By expanding T^4 using Taylor's series approach about a free stream temperature T_∞. The two-dimensional electrical magnetohydrodynamic (EMHD) boundary layer flow equation of an incompressible electrical conducting nanofluid isas given as

Continuity Equation:

$$\frac{\partial u}{\partial x}+\frac{\partial v}{\partial y}=0 \tag{1}$$

Momentum Equation:

$$u\frac{\partial u}{\partial x}+v\frac{\partial u}{\partial y}=-\frac{1}{\rho_f}\frac{\partial P}{\partial y}+\nu\left(\frac{\partial^2 u}{\partial x^2}+\frac{\partial^2 u}{\partial y^2}\right)+\frac{\sigma}{\rho_f}\left(E(x)B(x)-B^2(x)u\right) \tag{2}$$

$$u\frac{\partial v}{\partial x}+v\frac{\partial v}{\partial y}=-\frac{1}{\rho_f}\frac{\partial P}{\partial y}+\nu\left(\frac{\partial^2 v}{\partial x^2}+\frac{\partial^2 v}{\partial y^2}\right)+\frac{\sigma}{\rho_f}\left(E(x)B(x)-B^2(x)v\right) \tag{3}$$

Energy Equation:

$$u\frac{\partial T}{\partial x}+v\frac{\partial T}{\partial y}=\frac{k}{\rho c_p}\left(\frac{\partial^2 T}{\partial x^2}+\frac{\partial^2 T}{\partial y^2}\right)+$$

$$\tau\left\{D_B\left(\frac{\partial C}{\partial x}\frac{\partial T}{\partial x}+\frac{\partial C}{\partial y}\frac{\partial T}{\partial y}\right)+\frac{D_T}{T_\infty}\left[\left(\frac{\partial T}{\partial x}\right)^2+\left(\frac{\partial T}{\partial y}\right)^2\right]\right\} \tag{4}$$

$$+\frac{16\sigma^* T_\infty^3}{3k^*\rho c_p}\frac{\partial^2 T}{\partial y^2}+\frac{\mu}{\rho c_p}\left(\frac{\partial u}{\partial y}\right)^2+\frac{\sigma}{\rho c_p}\left(uB(x)-E(x)\right)^2$$

Mass diffusion Equation:

$$u\frac{\partial C}{\partial x}+v\frac{\partial C}{\partial y}=D_B\left(\frac{\partial^2 C}{\partial x^2}+\frac{\partial^2 C}{\partial y^2}\right)+\frac{D_T}{T_\infty}\left(\frac{\partial^2 T}{\partial x^2}+\frac{\partial^2 T}{\partial y^2}\right)-k_r^*(C-C_\infty) \tag{5}$$

The corresponding boundaryconditions are:

$$y=A(x+b)^{\frac{(1-n)}{2}}, u=U_w(x)=U_0(x+b)^2, v=0, T=T_\infty, C=C_w$$
$$y\to\infty: u\to 0, T\to T_\infty, C\to C_\infty \tag{6}$$

In this equations, x and y are the coordinates axis, $B(x)=B_0(x+b)^{(n-1)/2}$ is the magnetic function, σ is the electrical conductivity, $E(x)=E_0(x+b)^{(n-1)/2}$ is the electrical field factor, ν,ρ_f are the kinematic viscosity of the fluid andthe fluid density. $\frac{k}{\rho c_p}, \mu, \sigma^*, \rho c_f$ and ρ_p is the thermal diffusivity, the kinematic viscosity, the Stefan-Boltzmann constant, the density, the fluid density and particles density respectively.

Here $B_0, D_B, D_T, \tau = (\rho c)_p / (\rho c)_f$ represents the magnetic field, the Brownian diffusion coefficient, the thermophoresisdiffusion coefficient, the ratio between the effectiveheat transfer capacities of the nanoparticle materialand the heat capacity of the fluid flow. Here*A*is the stretching sheet constant, b is the stretching rate and w is the wall notation.

For the problem, we introduce the similarity transformations as follows:

$$\psi = \left(\frac{2}{n+1} v U_0 (x+b)^n\right)^{1/2} G(\xi), \xi = y\left(\frac{n+1}{2v} U_0 (x+b)^{n-1}\right)^{1/2},$$
$$\theta(\eta) = (T - T_\infty)/(T_w - T_\infty), \phi(\eta) = (C - C_\infty)/(C_w - C_\infty), \quad (7)$$
$$u = U_0 (x+b)^n G(\xi), v = -\left(\frac{n+1}{2} v U_0 (x+b)^{n-1}\right)^{1/2} \left(G(\xi) + \xi \frac{n-1}{n+1} G'(\xi)\right)$$

Using an order magnitude analysis of the y – directionmomentum equation applyingthe normal boundary layer equation as $u >> v$

$$\frac{\partial u}{\partial y} >> \frac{\partial u}{\partial x}, \frac{\partial v}{\partial x} >> \frac{\partial v}{\partial y} \text{ and } \frac{\partial p}{\partial y} = 0 \quad (8)$$

After employing the boundary layer approximation stated in (8), substitute the equation (7) into equations (1)–(3), we obtained the transformedordinary differential equation as:

$$G'''(\xi) + G(\xi) G''(\xi) - \frac{2n}{n+1}\left(G'(\xi)\right)^2 + M\left(E_1 - G'(\xi)\right) = 0 \quad (9)$$

Here $G(\xi)$ is the dimensionless velocity with the followingboundary conditions:

$$\xi = 0 : \mathrm{G}(\xi) = \alpha \frac{1-n}{1+n}, \mathrm{G}'(\xi) = 1 \text{ and } \xi \to \infty : \mathrm{G}'(\xi) = 0 \quad (10)$$

In a similar way the same is applicable to the equations (4) and (5). where $\alpha = A\left(\frac{n+1}{2}\frac{U_0}{v}\right)^{1/2}$

Let us consider $G(\xi) = f(\xi - \alpha) = f(\eta)$. The above equation (1)–(9) becomes:

$$f'''(\eta) + f(\eta) f''(\eta) - \frac{2n}{n+1}\left(f'(\eta)\right)^2 + M\left(E_1 - f'(\eta)\right) = 0 \quad (11)$$

$$\left(1 + \frac{4}{3}R\right)\theta'' + \mathrm{Pr}\left(f\theta' + Nb\phi'\theta' + Nt\theta'^2 + Ec\left(f''\right)^2 + MEc\left(f' - E_1\right)^2\right) = 0 \quad (12)$$

$$\phi'' + \frac{Nt}{Nb}\theta'' + Lef\phi' - Le\gamma\phi = 0 \quad (13)$$

Subject to the boundary conditions:

$$\eta = 0 : f(\eta) = \alpha \frac{1-n}{1+n}, f'(\eta) = 1, \theta(\eta) = 1, \phi(\eta) = 1$$
$$\eta \to 0 : f'(\eta) = 0, \theta(\eta) = 0, \phi(\eta) = 0 \quad (14)$$

where the primes denote differentiation with respect to η, f is the function related to the velocity field, θ- the dimensionless temperature and ϕ- the concentration of flow field, α is the wall thickness parameter, $M = 2\sigma B_0^2 / \rho_f U_0 (n+1)$ is the magnetic field parameter, $E_1 = E_0 / B_0 U_0 (x+b)^n$ is the electric parameter. $\mathrm{Pr} = \mu c_p / k$ is the Prandtl number, $Nb = (\rho c)_p D_B (C_w - C_\infty)/(\rho c)_f \nu$ is the Brownian motion parameter, $Le = \nu / D_\mathbf{B}$ is the

Lewis number, $Nt = (\rho c)_p D_T (T_w - T_\infty)/(\rho c)_f \nu T_\infty$ is the thermo phoresis parameter, $Ec = U_w^2 / c_p (T_w - T_\infty)$ is the Eckert number, and $R = 4\sigma^* T_\infty^3 / k^* k$ is the radiation parameter respectively.

TheBrownian motion is made of a different composition of factor values such as $(\rho c)_p, (\rho c)_f, D_B, C_w, C_\infty, \nu$ and involved of thegoverning equation under investigation. Here k_f, k_p are the thermal conductivities of the base fluid and nanoparticle, $\gamma = 2k^*/(n+1)U_0 (x+b)^{n-1}$ is the chemical reaction parameter. The c_f is skin friction coefficient defined in terms of shear stress, q_W is the wall heat flux and q_m is the wall mass fluxdefined as:

$$c_f = \frac{\tau_w}{\rho U_w^2(x)}, q_w = -\left(k + \frac{16\sigma^* T_\infty^3}{3k^*}\right)\frac{\partial T}{\partial y}\bigg|_{y=A_1(x+b)^{\frac{1-n}{2}}}, q_m = -D_B \frac{\partial \phi}{\partial y}\bigg|_{y=A_1(x+b)^{\frac{1-n}{2}}} \quad (15)$$

where τ_w is the surface shear stress expressed in terms of μ dynamic viscosity of the fluid stretching surface defined as

$$\tau_w = \mu \frac{\partial u}{\partial y}\bigg|_{y=A_1(x+b)^{\frac{1-n}{2}}}, Nu_x = (x+b)^{\frac{1-n}{2}} q_w / k(T_w - T_0), Sh_x = (x+b)^{\frac{1-n}{2}} q_m / D_B(\phi_w - \phi_0) \quad 16)$$

The local skin-friction coefficient, Nusselt number andSherwood number are presented in a non-dimensional form as:

$$\mathrm{Re}_x^{1/2} c_{fx} = \sqrt{\frac{1+n}{2}} f''(0), Nu_x (\mathrm{Re}_x)^{-1/2} = -\left(1 + \frac{4}{3}R\right)\sqrt{\frac{1+n}{2}}\theta'(0),$$
$$Sh_x / \mathrm{Re}_x^{1/2} = -\sqrt{\frac{1+n}{2}}\theta', \quad (17)$$

Here $\mathrm{Re}_x = U_w(x+b)/\nu$ is the local Reynolds number.

NUMERICAL PROCEDURE

The similarity transformation converts the non-linear partial differential Equations (2)-(5) into ordinary differential equations. The set of nonlinear ordinary differential equations (11)-(13) with the corresponding boundary conditions in (14) have been solved numerically using the method of Runge-Kutta forth order along with shooting technique implemented in MATLAB software.

RESULTS AND DISCUSSION

In order toget a clear insight of the physical problem, the numerical computations have been carried out using the method described in the previous section for the various values of different parameters such as the magnetic parameter

Figure 2 exhibit the concentration profiles of nanofluid for different values of chemical reaction parameter. It is noticed thatthe chemical reaction parameter decreases, the nanoparticle concentration decreases. the concentration profile and solutal boundarylayer thickness decreases. This induces the mass transfer toreduce for decrease for high values of chemical reactionparameter. High values of wall thickness parameter reducethe fluid concentration and solutal boundary layer thickness. The rate of mass transfer reduces at the surface of the stretchingsheet for a high rate of chemical reactionincreasing the values of chemical reaction parameter, the concentration profiles decreases. The various values of

Lewis number (Le) on concentration is plotted in Figure 3. As the Lewis number increase the concentration profiles decreases.

The reason is that mass transfer rate is sensitive to an increasing values of Lewis number. It also observed that the Sherwood number at the surface decreases. Moreover, the concentration of the nanofluid at the surface reduces more compared to the absence of wall thickness as the values of Lewis number increases.

Figure 4 demonstrate the effects of thermophoresis parameter on the concentration profiles of the fluid. The effect of thermophoresis parameter increases which results the concentration of the fluid increases, it is since the values of solutal boundary layer thickness become thicker and the concentration field increases. In figure 5, it is viewed that Brownian motion parameter shows decreasing effects on nano particle volume fraction. As the value of Nb increases the solutal boundary layer thickness is decreasing, it results the fall in concentration. Soret number increase in the Brownian motion of the fluid leads to decrease in the concentration profiles. Figure 6 depicts the influence of electric field on the concentration profiles of the fluid, for higher values of an electric field parameter the solutal boundary layer thickness decreases, and concentration of the fluid decreased.

Figure 7 describes the influence of electric field on the velocity of the fluid, the velocity of the nano fluid increases with increase value of the electric field. Figure 8 portray the effect of electric field parameter on temperature profiles. As the electric field parameter values E increased the temperature profiles are increasing. Figure 9 depicts the magnetic field influences on the velocity of the nano fluid. The fluid velocity reduced with increment of magnetic parameter M. The magnetic parameter defines the ratio of Lorentz force to the viscous force. Therefore, large values of M enhance the Lorentz force, this force produces more resistance to the transport phenomena due to which the velocity of the fluid reduces. Figure 10 shows the effect of non-linear stretching parameter on the velocity profiles. It is observed that velocity of the nano fluid enhancing when increasing the non-linear stretching parameter.

Figure 11 demonstrates the effects of thermal radiation on temperature profiles. It is found that the radiation parameter increases then fluid temperature increases monotonically. The rate of heat transfer at the surface reduces for higher thermal radiation effects. Higher values of radiation parameter lead to low rate of heat transfer at the surface why because the nano fluid temperature is enhanced. Figure 12 demonstrates how wall thickness effects the velocity profiles. The fluid velocity reduces on enhancing the wall thickness because the thickness of momentum boundary layer becomes thinner for higher values of wall thickness parameter and reduces velocity profiles. Figure 13 portray the effect of Prandtl number on temperature of the nano fluid. Increasing the Pr number reduces the thermal boundary layer thickness and temperature of the nano fluid because Prandtl number is the ratio of momentum diffusivity to thermal diffusivity. When thermal diffusivity is decreases, automatically Prandtl number increases and the temperature of the fluid decreases. In other words, Prandtl number and temperature have an inverse relation. Prandtl number controls the relative thickness of the momentum boundary layer and thermal boundary layer. One can easily control or predict the temperature.

Table1 shows that the skin-friction, Nusselt number and Sherwood number for different values pertinent parameters like, γ, *Le, Nt, Nb, R, Pr, n,* and M. It is observed that all the parameters are increases, the skin-friction, Nusselt number and Sherwood number are increased.

Figures

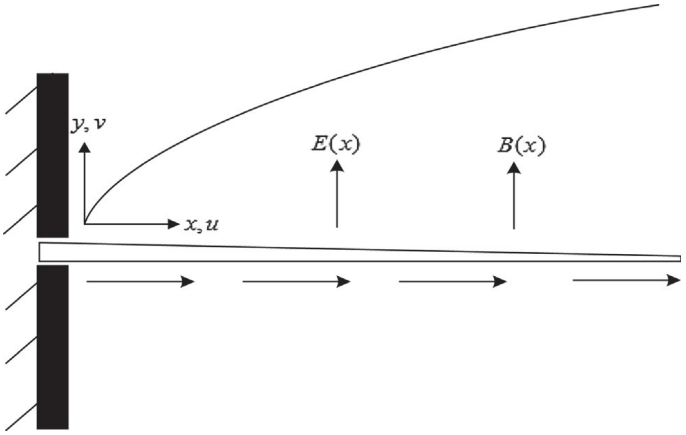

Figure. 1 Physical configuration of the geometry.

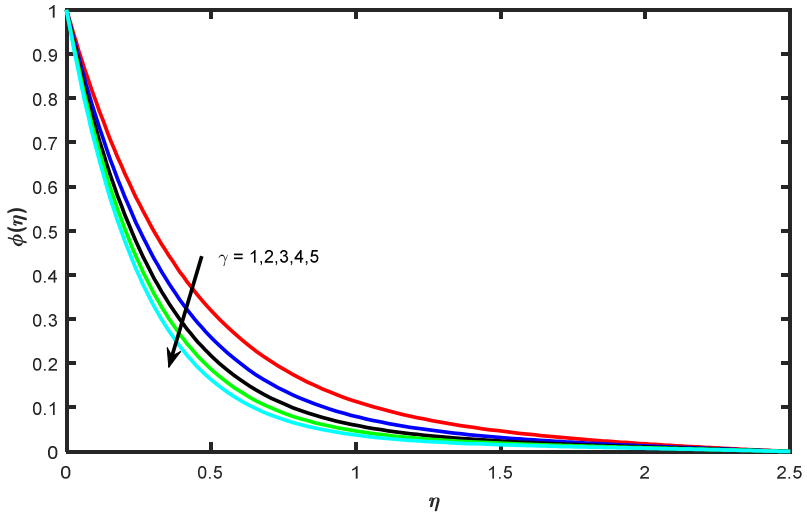

Figure 2.Concentration profiles for different values of chemical reaction parameter (γ).

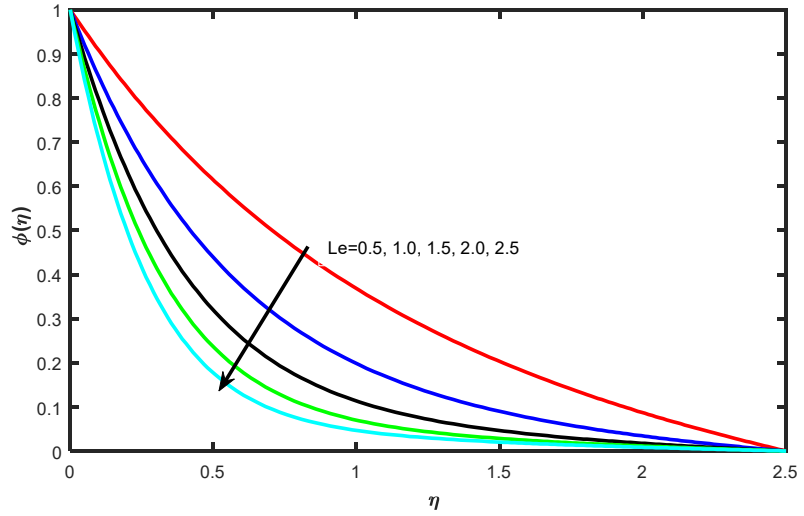

Figure 3. Concentration profiles for different values of Lewis number (Le).

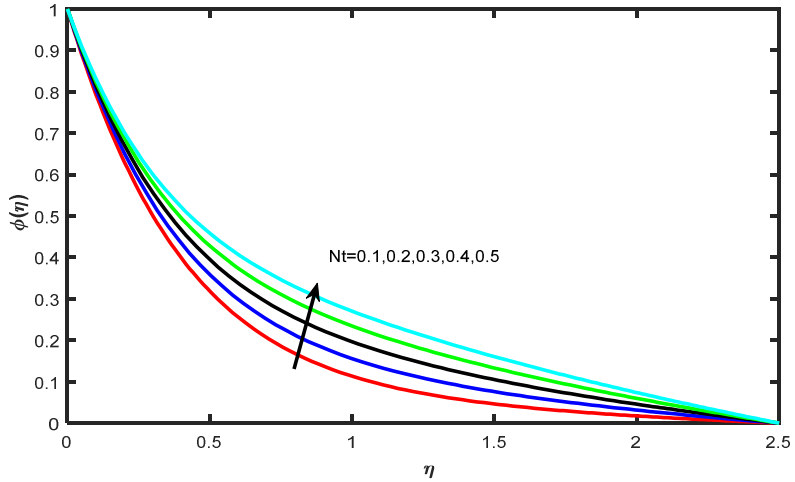

Figure 4. Concentration profiles for different values of thermophoresis parameter (Nt).

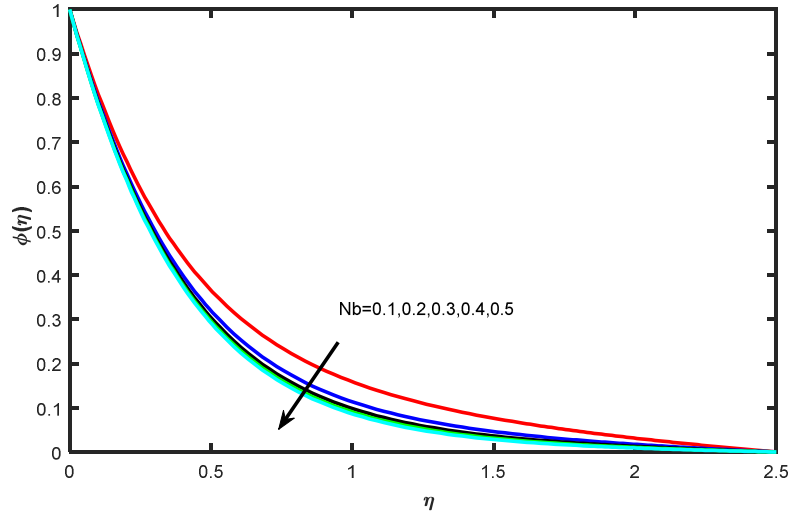

Figure 5.Concentration profiles for different values of Brownian parameter (Nb).

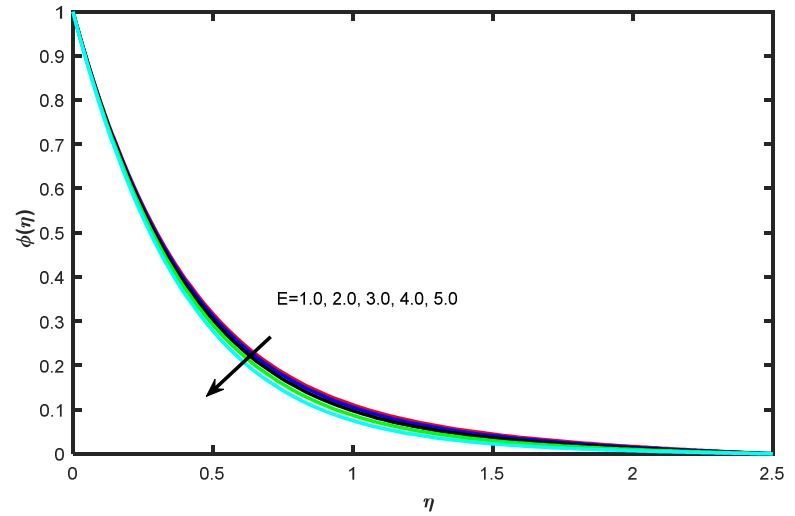

Figure 6.Concentration profiles for different values of electric parameter (E).

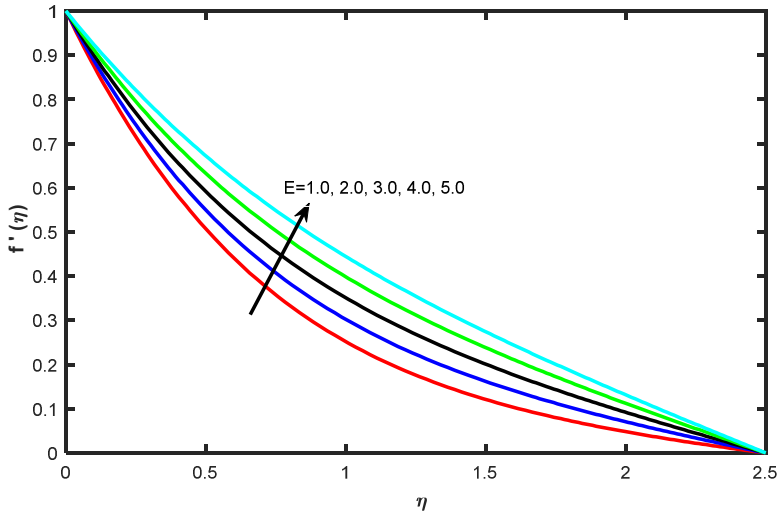

Figure 7.Velocity profiles for different values of electric parameter (E).

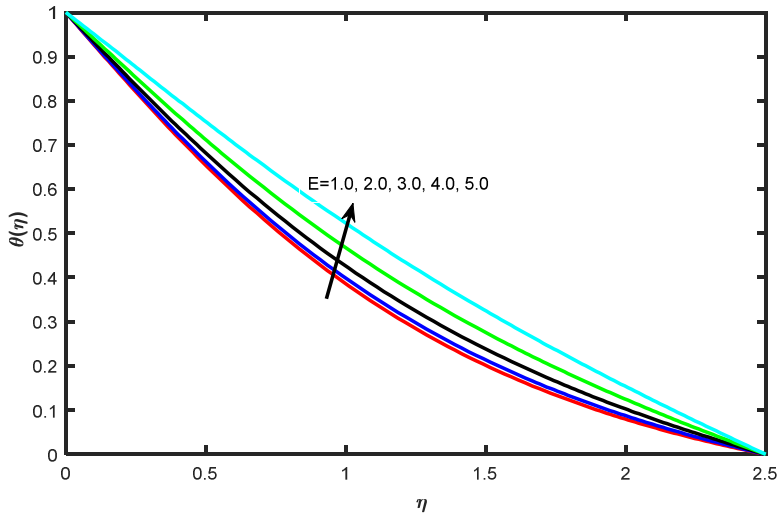

Figure 8.Temperature profiles for different values of electric parameter (E).

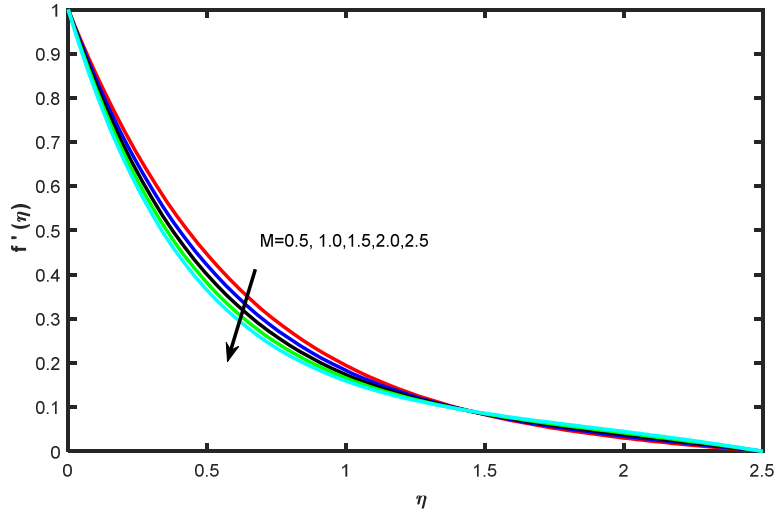

Figure 9.Velocity profiles for different values of magnetic parameter (M).

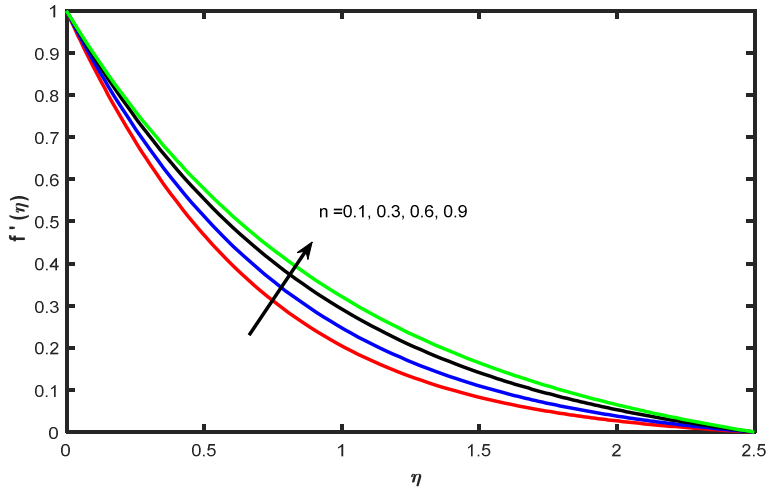

Figure 10.Velocity profiles for different values of non-linear stretching parameter (n).

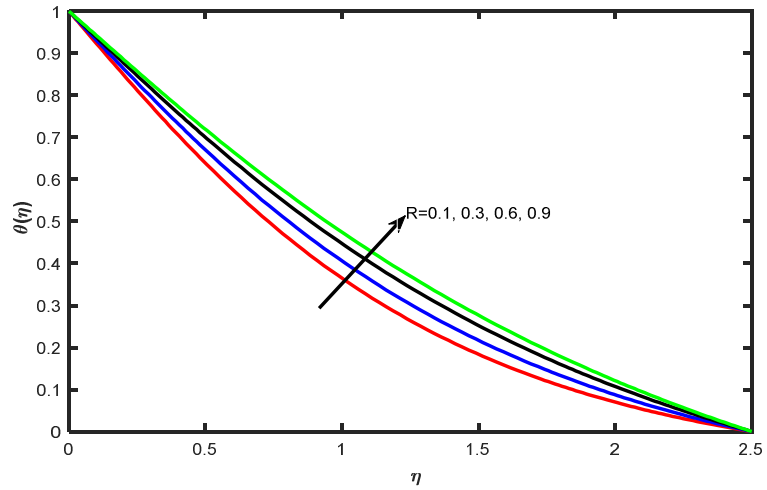

Figure 11.Temperature profiles for different values of thermal radiation parameter (R).

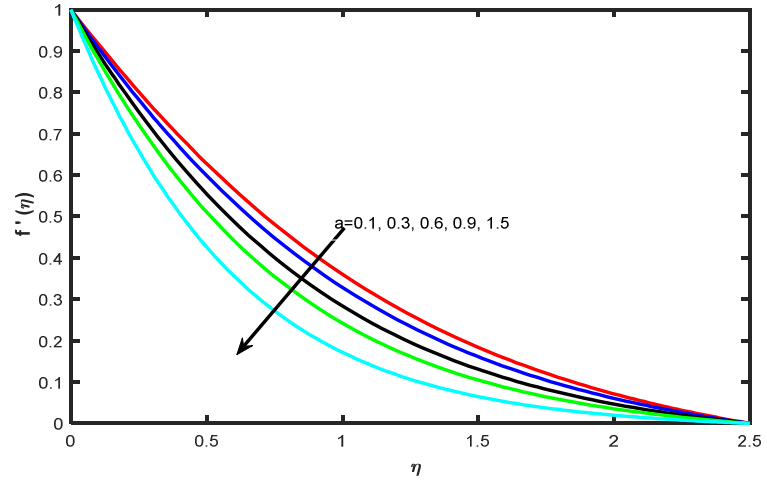

Figure 12.Velocity profiles for different values of wall thickness parameter (a).

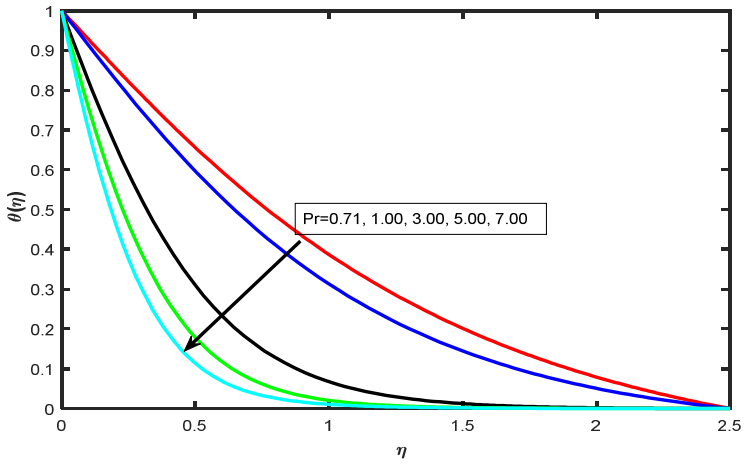

Figure 13. Temperature profiles for different values of Prandtl number (Pr).

Table 1

Table-1											
γ	**Le**	**Nt**	**Nb**	**R**	**Pr**	**n**	**a**	**M**	**SF**	**Nu**	**Sh**
1	1.5	0.1	0.2	0.2	0.71	0.1	1.2	0.1	1.439421	0.711056	2.280228
2	1.5	0.1	0.2	0.2	0.71	0.1	1.2	0.1	1.439421	0.712106	2.717276
3	1.5	0.1	0.2	0.2	0.71	0.1	1.2	0.1	1.439421	0.713466	3.073876
4	1.5	0.1	0.2	0.2	0.71	0.1	1.2	0.1	1.439421	0.715335	3.381855
5	1.5	0.1	0.2	0.2	0.71	0.1	1.2	0.1	1.439421	0.718154	3.656701
1	**0.5**	0.1	0.2	0.2	0.71	0.1	1.2	0.1	1.439421	0.711816	0.971500
1	**1**	0.1	0.2	0.2	0.71	0.1	1.2	0.1	1.439421	0.714390	1.651337
1	**1.5**	0.1	0.2	0.2	0.71	0.1	1.2	0.1	1.439421	0.718154	2.280228
1	**2**	0.1	0.2	0.2	0.71	0.1	1.2	0.1	1.439421	0.724124	2.876273
1	**2.5**	0.1	0.2	0.2	0.71	0.1	1.2	0.1	1.439421	0.734560	3.450751
1	1.5	**0.1**	0.2	0.2	0.71	0.1	1.2	0.1	1.439421	0.647189	1.885596
1	1.5	**0.2**	0.2	0.2	0.71	0.1	1.2	0.1	1.439421	0.664245	1.962453
1	1.5	**0.3**	0.2	0.2	0.71	0.1	1.2	0.1	1.439421	0.681749	2.053449
1	1.5	**0.4**	0.2	0.2	0.71	0.1	1.2	0.1	1.439421	0.699714	2.159171
1	1.5	**0.5**	0.2	0.2	0.71	0.1	1.2	0.1	1.439421	0.718154	2.280228
1	1.5	0.1	**0.1**	0.2	0.71	0.1	1.2	0.1	1.439421	0.628675	2.114032
1	1.5	0.1	**0.2**	0.2	0.71	0.1	1.2	0.1	1.439421	0.657408	2.280228
1	1.5	0.1	**0.3**	0.2	0.71	0.1	1.2	0.1	1.439421	0.687225	2.335263
1	1.5	0.1	**0.4**	0.2	0.71	0.1	1.2	0.1	1.439421	0.718154	2.362514
1	1.5	0.1	**0.5**	0.2	0.71	0.1	1.2	0.1	1.439421	0.750224	2.378657
1	1.5	0.1	0.2	0.2	0.71	**1**	1.2	0.1	0.784558	0.484939	2.283555
1	1.5	0.1	0.2	0.2	0.71	**2**	1.2	0.1	0.913710	0.591564	2.299644
1	1.5	0.1	0.2	0.2	0.71	**3**	1.2	0.1	1.044987	0.668150	2.328434
1	1.5	0.1	0.2	0.2	0.71	**4**	1.2	0.1	1.178562	0.714491	2.369621
1	1.5	0.1	0.2	0.2	0.71	**5**	1.2	0.1	1.314634	0.730310	2.422951

1	1.5	0.1	0.2	0.2	0.71	0.1	1.2	0.1	1.568343	0.633219	2.282816
1	1.5	0.1	0.2	0.2	0.71	0.1	1.2	0.1	1.716827	0.648257	2.285951
1	1.5	0.1	0.2	0.2	0.71	0.1	1.2	0.1	1.853828	0.664441	2.288990
1	1.5	0.1	0.2	0.2	0.71	0.1	1.2	0.1	1.981382	0.682001	2.291943
1	1.5	0.1	0.2	0.2	0.71	0.1	1.2	0.1	2.101010	0.701250	2.294819
1	1.5	0.1	0.2	0.2	0.71	**0.1**	1.2	0.1	1.079806	0.449902	1.498230
1	1.5	0.1	0.2	0.2	0.71	**0.3**	1.2	0.1	1.149798	0.513499	1.683169
1	1.5	0.1	0.2	0.2	0.71	**0.6**	1.2	0.1	1.279903	0.613580	1.975420
1	1.5	0.1	0.2	0.2	0.71	**0.9**	1.2	0.1	1.439421	0.718154	2.280228
1	1.5	0.1	0.2	**0.1**	0.71	0.9	1.2	0.1	1.439421	0.571578	2.262241
1	1.5	0.1	0.2	**0.3**	0.71	0.9	1.2	0.1	1.439421	0.614476	2.294619
1	1.5	0.1	0.2	**0.6**	0.71	0.9	1.2	0.1	1.439421	0.684284	2.324349
1	1.5	0.1	0.2	**0.9**	0.71	0.9	1.2	0.1	1.439421	0.760527	2.342692
1	1.5	0.1	0.2	0.9	0.71	0.9	**0.1**	0.1	0.842616	0.470318	1.517350
1	1.5	0.1	0.2	0.9	0.71	0.9	**0.3**	0.1	0.937576	0.510903	1.643146
1	1.5	0.1	0.2	0.9	0.71	0.9	**0.6**	0.1	1.091954	0.575534	1.843371
1	1.5	0.1	0.2	0.9	0.71	0.9	**0.9**	0.1	1.259684	0.644644	2.056202
1	1.5	0.1	0.2	0.9	0.71	0.9	1.2	0.1	1.629668	0.795924	2.514098
1	1.5	0.1	0.2	0.9	0.71	0.9	1.2	0.1	1.439421	0.718154	1.112854
1	1.5	0.1	0.2	0.9	**1**	0.9	1.2	0.1	1.439421	0.866871	1.439678
1	1.5	0.1	0.2	0.9	**3**	0.9	1.2	0.1	1.439421	1.824713	1.799578
1	1.5	0.1	0.2	0.9	**5**	0.9	1.2	0.1	1.439421	2.606910	2.217112
1	1.5	0.1	0.2	0.9	**7**	0.9	1.2	0.1	1.439421	3.297355	2.280228

REFERENCES

[1]. Choi SUS. Enhancing thermal conductivity of fluid with nanoparticles, developments and applications of non-Newtonian flow. ASME FED 1995; 231:99–105.

[2]. Hayat T, Mehmood OU. Slip effects on MHD flow of third order fluid in planar channel. Commun Nonlinear SciNumerSimul 2013; 16(3):1363–77.

[3]. Nadeem S, Hussain M, Naz M. MHD stagnation flow of a micropolar fluid through a porous medium. Int J Meccanica 2010; 45:869–80.

[4]. KJha B, Apere CA. Unsteady MHD two phase Couette flow of fluid-particle suspension. Appl Math Model 2013; 37:1920–31.

[5]. Makinde OD, Chinyoka T. MHD transient flow and heat transfer of dusty fluid in channel with variable physical parameters and Navier slip boundary condition. Comput Math Appl 2010; 60:660–9.

[6]. T. Hayat, F. Shah, A. Alsaedi, and M. I. Khan, "Development of homogeneous/heterogeneous reaction in flow based through non-Darcy Forchheimer medium," Journal of Theoretical and Computational Chemistry, p. 1750045, 2017.

[7]. T. Hayat, M. W. A. Khan, A. Alsaedi, and M. I. Khan, "Squeezing flow of second grade liquid subject to non-Fourier heat flux and heat generation/absorption," Colloid and Polymer Science, vol. 295, no. 6, pp. 967-975, 2017.

[8]. M. I. Khan, T. Hayat, M. I. Khan, and A. Alsaedi, "A modified homogeneous heterogeneous reactions for MHD stagnation flow with viscous dissipation and Joule heating," International Journal of Heat and Mass Transfer, vol. 113, pp. 310-317, 2017.

[9]. T. Fang, J. Zhang, and Y. Zhong, "Boundary layer flow over a stretching sheet with variable thickness," Applied Mathematics and Computation, vol. 218, no. 13, pp. 7241-7252, 2012.

[10]. T. Hayat, M. I. Khan, M. Farooq, A. Alsaedi, M. Waqas, and T. Yasmeen, "Impact of Cattaneo–Christov heat flux model in flow of variable thermal conductivity fluid over a variable thicked surface," International Journal of Heat and Mass Transfer, vol. 99, pp. 702-710, 2016.

[11]. T. Hayat, M. I. Khan, A. Alsaedi, and M. I. Khan, "Homogeneous-heterogeneous reactions and melting heat transfer effects in the MHD flow by a stretching surface with variable thickness," Journal of Molecular Liquids, vol. 223, pp. 960-968, 2016.

[12]. M. I. Khan, M. I. Khan, M. Waqas, T. Hayat, and A. Alsaedi, "Chemically reactive flow of Maxwell liquid due to variable thicked surface," International Communications in Heat and Mass Transfer, vol. 86, pp. 231-238, 2017.

[13]. M. W. A. Khan, M. Waqas, M. I. Khan, A. Alsaedi, and T. Hayat, "MHD stagnation point flow accounting variable thickness and slip conditions," Colloid and PolymerScience, pp. 1-9, 2017.

[14]. M. Waqas, M. I. Khan, T. Hayat, A. Alsaedi, and M. I. Khan, "Nonlinear thermal radiation in flow induced by a slendering surface accounting thermophoresis andBrownian diffusion," The European Physical Journal Plus, vol. 132, no. 6, p. 280, 2017.

[15]. M. I. Khan, T. Hayat, M. Waqas, M. I. Khan, and A. Alsaedi, "Impact of heatgeneration/absorption and homogeneous-heterogeneous reactions on flow of Maxwellfluid," Journal of Molecular Liquids, vol. 233, pp. 465-470, 2017.

[16]. T Hayat, M Waqas, S A Shehzad and S Alsaed, Stretched flow of Carreau nanofluid with convective boundary condition, PRAMANA-Journal of Physics, 86 (2016) 3-17.

[17]. Syahira Mansur and AnuarIshak,. The flow and heat transfer of a nanofluid past a stretching/shrinking sheet with a convective boundary condition, Abstract and Applied Analysis, Volume 2013,

[18]. A. Malvandi and D. D. Ganji, Brownian motion and thermophoresis effects on slip flow of alumina/water nanofluid inside a circular microchannel in the presence of a magnetic field, International Journal of Thermal Sciences**,** 84 (2014) 196-206.

[19]. B. Mahanthesh, F. Mabood, B.J. Gireesha and R.S.R. Gorla, Effects of chemical reaction and partial slip on the three-dimensional flow of a nanofluid impinging on an exponentially stretching surface, The European Physical Journal Plus, Eur. Phys. J. Plus 132 (3) (2017) 1-18.